https://doi.org/10.5194/wes-2020-20
Preprint. Discussion started: 31 March 2020

eawe european academy of wind energy
Open Access WIND ENERGY SCIENCE DISCUSSIONS

Development of a numerical model of a novel leading edge protection component for wind turbine blades

William Finnegan[1,2], Priya Dasan Keeryadath[3], Rónán Ó Coistealbha[3], Tomas Flanagan[3], Michael Flanagan[3], Jamie Goggins[1,2]

[1]Civil Engineering, School of Engineering, National University of Ireland Galway, H91 HX31, Ireland
[2]MaREI Centre, Ryan Institute, National University of Ireland Galway, H91 HX31, Ireland
[3]ÉireComposites Teo, An Choill Rua, Inverin, Co. Galway, H91 Y923, Ireland

Correspondence to: William Finnegan (william.finnegan@nuigalway.ie)

Abstract. As the world shifts to using renewable sources of energy, wind energy has been established as one of the leading forms of renewable energy. However, as wind turbines get increasingly larger, new challenges within the design, manufacture and operation of the turbine are presented. One such challenge is leading edge erosion on wind turbine blades. With larger wind turbine blades, tip speed begin to reach over 500 km per hour. As water droplets impact along the leading edge of the blade, rain erosion begins to occur, increasing maintenance costs and reducing the design life of the blade. In response to this, a new leading edge protection component (LEP) for offshore for wind turbine blades is being developed, which is manufactured from thermoplastic polyurethane. In this paper, an advanced finite element analysis (FEA) model of this new leading edge protection component has been developed. Within this study, the FEA model has been validated against experimental trials at demonstrator level, comparing the deflection and strains during testing and found to be in good agreement. The model is then applied to a full-scale wind turbine blade is then modelled with the LEP bonded onto the blade's leading edge and compared to previously performed experimental trials, where the results were found to be well aligned when comparing the deflections of the blade. The methodology used to develop the FEA model can be applied to other wind blade designs in order to incorporate the new leading edge protection component to eliminate the risk of rain erosion and improve the sustainability of wind turbine blade manufacture, while increasing the service life of the blade.

1 Introduction

In recent years, the global issue of climate change has come to the fore, along with the need to move towards a more sustainable way of living. With this move to sustainable living, the use of renewable energy becomes more prominent, where wind energy has established itself as one of the leading sources of renewable energy. By 2020, the global wind energy capacity is expected to almost double to reach a level of 650.8GW (Conway, 2015). As the wind energy industry grows, increasingly more wind farms are being developed offshore due to favourable social and environmental factors compared to onshore. With this development in the sector, wind turbine blades are now become much larger with the increased resource and the need for fewer

https://doi.org/10.5194/wes-2020-20
Preprint. Discussion started: 31 March 2020

eawe european academy of wind energy
Open Access WIND ENERGY SCIENCE DISCUSSIONS

turbines, where the average capacity of wind turbines installed in European waters has doubled, from 2MW in 2000 to 4MW in 2014 and SEIMENS Gamesa announced their 10MW (193 diameter wind turbine) this year (SEIMENS, 2019).

As the industry moves towards these larger wind turbine blades, a new challenge presents itself – with higher blade tip speeds, erosion along the leading edge due to the impact of rain droplets begins to occur at an accelerated rate. Leading edge rain erosion is one of the leading reasons for continuous maintenance of the surface of wind turbine blade. As wind turbines move offshore, the cost of maintenance increases ten-fold, due primarily to accessibility difficulties. Additionally, rain erosion along the leading edge of the blades reduces a wind turbine's annual energy production by between 2% and 25% (Budinski, 2007).

Currently, a number of leading edge protection methods are available, which are applied to wind turbine blades at the end of their manufacture, including tapes, paints and coatings (Chen et al., 2019). In 2013, a comprehensive review, which details these methods along with a number of other techniques for preventing erosion on the leading edge erosion of wind turbine blades, was compiled by Keegan at al. (2013). Additionally, Dashtkar et al. (2019) reviewed the liquid erosion mechanism, water erosion testing procedures and the contributing factors to the erosion of the leading edge of wind turbine blades, including a brief discussion on the use of carbon nanotubes and graphene nano-additives for improving the erosion resistance of the leading edge. Initially, the protective coatings were made from epoxy or polyester but over time, these rigid coatings were found to be inadequate and more ductile materials, such as polypropylene and polyurethane, were necessary. In recent years, manufacturers have moved towards multi-layered solutions, which can be designed to optimise performance and as a means of assessing the durability of the protection system. In general, leading edge protection methods can be divided into two categories: in-mould and post-mould solutions (Cortés et al., 2017; Keegan et al., 2013). The in-mould solutions are applied directly to the matrix substrate, using painting or spraying. These coating are typically rigid, brittle and have a high modulus, compared to the more flexible coatings, such as polyurethane (Keegan et al., 2013), that are used for the post-mould solutions. The post-mould protective systems are typically multi-layer systems with the inclusion of filler and primer layers between the laminate substrate and surface coating. These methods provide additional protection from erosion during operation, but usually require replacement during the service life of the wind turbine blade. However, this replacement becomes more regular in larger wind turbine blades and, thus, increasingly costly with the need for this additional maintenance.

In recent years, finite element analysis (FEA) has come to the fore for the design and development of composite wind turbine blades. Chezly (1993) developed a software, based on the finite element method, to perform a static and dynamic analysis of wind turbine blades and found that the maximum stresses occurred at the root of the blades for all configurations in the spanwise direction. Commercial software, with additional routines or modules developed as an add-on, have been used to perform an advanced FEA of composite wind turbine blades. Barnes et al. (2015) used a FEA, in ANSYS, to demonstrate the use of an improved design method specifically for low wind speed blades. During the analysis, the strength constraint imposed was the Tsai–Wu failure criterion in order to determine the optimum structural design for the spar caps and webs of two wind turbine blades. Yeh and Wang (2017) used the finite element analysis software ANSYS to perform a stress analysis of a 5 MW composite wind turbine blade, where they found that the largest combined load occurred at a 0° pitch angle and the stress and displacement are the greatest when the wind blade is located at 120° angular position from its highest vertex. Zhu and Rustamov

https://doi.org/10.5194/wes-2020-20
Preprint. Discussion started: 31 March 2020

(2013) performed a structural analysis, using the finite element method, to evaluate a 750 kW wind turbine blade under various load conditions. Zhou et al. (2016) also used the finite element analysis software ABAQUS to explore the performance of a wind turbine blade and perform a modal analysis. Fagan et al. (2017) performed a FEA, using the finite element analysis software ABAQUS, which incorporated a design optimisation genetic algorithm, on a 13m wind turbine blade. The genetic algorithm resulted in five optimal blade designs, showing a reduction in mass up to 24%. Tarfaoui et al. (2019) used the finite element analysis software ABAQUS to localize the susceptible sections of a full-scale 48 m fiberglass composite offshore wind turbine blades under operational conditions.

Therefore, in this paper, a FEA model of a new wind turbine blade component (LEP) attached to the leading edge of a full-scale wind turbine blade has been developed. The LEP has been designed to protect the leading edge of a wind turbine blade from rain erosion, particularly in the offshore environment. The development details for the FEA model are defined, along with a validation study of the model with the experimental structural static testing of a representative leading edge demonstrator. The validated FEA model has then been applied to a full-scale wind turbine blade with the LEP bonded to the leading edge. Additionally, the effect of the LEP on the structural performance of wind turbine blade has been analysed and discussed.

2 Materials and methods

2.1 Aim and objectives

The overall aim of this report is to develop a finite element model of a novel leading edge protection component (LEP) that is bonded to a wind turbine blade. The purpose of the model is to assist engineers when incorporating the LEP in the design of their wind turbine blades. However, in order to achieve the aim of the study, a number of objectives must be achieved:

- To develop a validated wind turbine blade FEA model
- To incorporate the LEP into the model
- To validate the accuracy of the FEA model using experimental trials through structural testing

2.2 Methodology

In this paper, a numerical FEA model of a new wind turbine component, LEP, which protects the leading edge of a wind turbine blade, is being developed. Further details on the development of the LEP can be found in Finnegan et al. (2020). The analysis used in this study is based on the proposed test pyramid by Lopes et al. (Lopes et al., 2016), which is summarised graphically in Figure 1.

https://doi.org/10.5194/wes-2020-20
Preprint. Discussion started: 31 March 2020

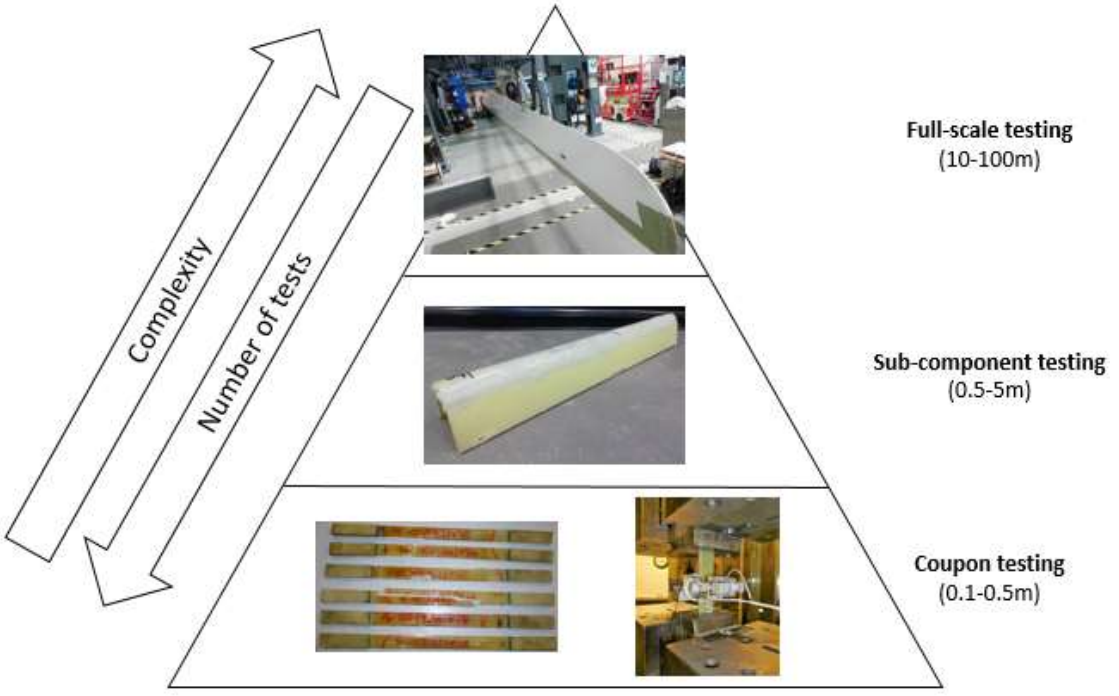

Figure 1: Test pyramid methodology for the development of a new wind turbine blade component that is used in this study

2.3 Governing equations

The FEA model has been developed using ANSYS WorkBench 17.1 (ANSYS, 2017), where it will combine a number of the ANSYS software packages, including DesignModeler and Mechanical (ADPL). The ADPL solver is based on the finite element method, where ADPL incorporates the layup details of the composite material substrate that makes up the majority of the wind turbine blade structure.

2.4 Materials

The materials used in the current study are defined in the numerical model using their material properties, which are summarised in Table 1. The composite material used in this study is glass-fibre reinforced powder epoxy and the material properties for unidirectional (UD), bi-axial (BIAX) and tri-axial (TRIAX) fibre orientations are given in Table 1, along with the lightweight polyurethane (PU) core that is used in the wind blade manufacture. The material properties for the LEP, which is manufactured from a novel thermoplastic polyurethane material, is also given in Table 1.

https://doi.org/10.5194/wes-2020-20
Preprint. Discussion started: 31 March 2020

105

Table 1: Material properties for the thermoplastic and composite materials used in the current study

	UD	BIAX	TRIAX	PU Core	LEP
E_1 (MPa)	38,800[1]	22,293	25,800	10	560
E_2 (MPa)	12,950[2]	22,293	17,500	10	560
G_{12} (MPa)	3,670	3,670	3,670	3,846	373
v_{12}	0.3	0.3	0.3	0.3	0.25
Density (kg/m^3)	1,200	1,200	1,200	80	950

[1] Calculated from testing results to ISO 527, where the tensile modulus is 39,700MPa and the compressive modulus is 37,900MPa

[2] Calculated from testing results to ISO 527, where the tensile modulus is 11,900MPa and the compressive modulus is 14,000MPa

110

3 Model development

3.1 Coupon testing and modelling

3.1.1 Composite test specimen model

The first stage in the model development was the development of a FEA model of a composite test specimen. The use of composite materials within the FEA model presented the greatest challenge and made up the majority of the final model, by mass, as wind turbine blades are made of fibre-reinforced polymer composites. In this study, the composite sections of the wind turbine blade are modelled using shell elements in ANSYS DesignModeler and the plies are modelled using the "Layered Section" in ANSYS Mechanical ADPL. Composite material plies are defined by specifying the ply material properties, thickness and orientation. The resulting material properties of the part can then be used within the FEA solver. The Young's modulus of the ply (Eply) is estimated using the Rule of Mixtures (Agarwal et al., 2017), as follows:

$$E_{ply} = \kappa V_f E_f + V_m E_m \,, \tag{1}$$

where κ is a correction factor that accounts for the fibre area, the fibre diameter distribution, the interface and the fibre orientation distribution, V_f is the fibre volume faction (0.52), E_f is the Young's modulus of the fibre (72.4 GPa), V_m is the matrix volume fraction and E_m is the Young's modulus of the matrix (3.89 GPa). The FEA when loads are applied within the numerical composite material model is performed using ANSYS Mechanical Static Structural with ANSYS Workbench.

In order to validate the accuracy of this numerical composite material model, a validation study took place, where the results of the numerical model were compared to the results from physical testing of fibre-reinforced polymer composite specimens. The specimens were manufactured from E-glass bi-axial 45°/135° material (AHLSTROM 62042) that was prepared with a

https://doi.org/10.5194/wes-2020-20
Preprint. Discussion started: 31 March 2020

eawe european academy of wind energy
Open Access WIND ENERGY SCIENCE DISCUSSIONS

quasi-isotropic lay-up and infused with epoxy resin (Gurit's Ampreg 22 (Gurit)) with a slow hardener using the Vacuum Assisted Resin Transfer (VART) method at ÉireComposites Teo. The quasi-isotropic lay-up for 16 ply panels was specified as [(45°/135°, 0°/90°)2]s and the specimen was cured for 48 hours at room temperature (21°C), followed by a post cure at 75°C for 5 hours.

The static tensile testing was carried out in accordance with *ASTM D3039: Standard Test Method for Tensile Properties of Polymer Matrix Composite Materials* (ASTM, 2017) using a 250kN Zwick test machine with wedge grips, as shown in Figure 2 (a). The test composite specimens is loaded at a speed of 2mm/min and the stain is measured between 0.1-0.3% using a biaxial extensometer in order to calculate the Young's Modulus of the specimen. In total 5 specimens were tested. The results of this physical testing, including an upper and lower bound for the test results and the average based on the mean Young's Modulus from this physical testing (calculated to be 19,567.2 MPa for the material) are compared to the results from the numerical composite material model, which estimated the Young's Modulus of the material as 18,926.5 MPa. Therefore, the results are found to be in very good agreement, as shown in Figure 2 (b), with the numerical model underestimating by approximately 3% but very close to the results of one of the specimen physical tests. Therefore, this difference is well within the allowable experimental error expected for this study. The Young's Modulus obtained here is also in line with that of Kennedy et al. (Kennedy et al., 2018), who reported a value of 19,300 MPa for a similar epoxy infused E-glass material.

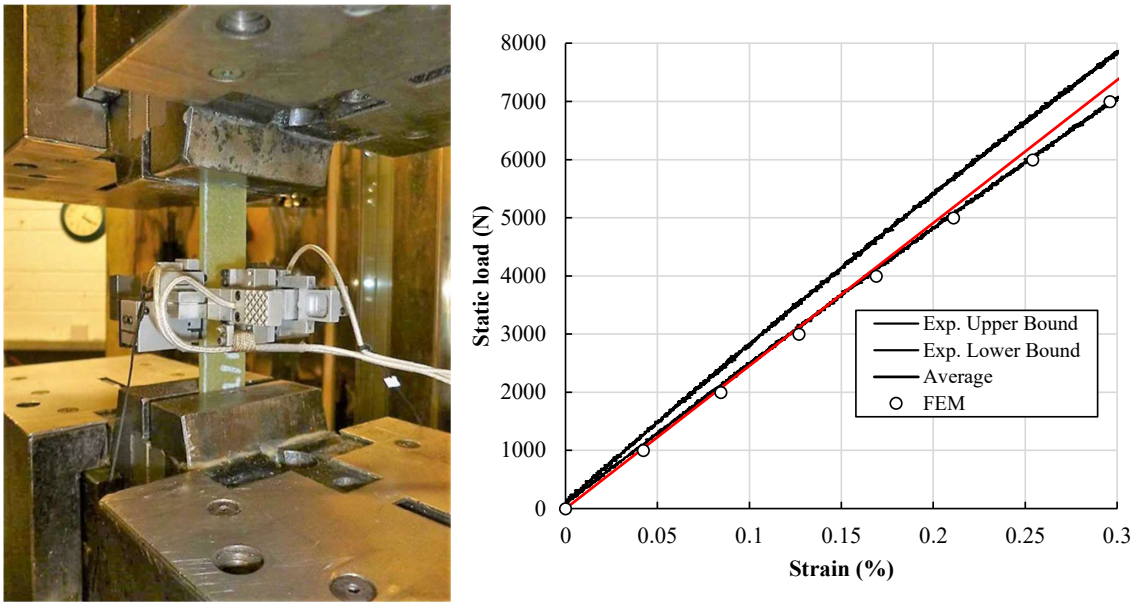

(a) (b)

Figure 2: Experimental static testing of glass-fibre reinforced specimens, where (a) is the tests being performed and (b) is a comparison of the experimental static testing results with the results from the FEA model

https://doi.org/10.5194/wes-2020-20
Preprint. Discussion started: 31 March 2020

eawe european academy of wind energy
Open Access WIND ENERGY SCIENCE DISCUSSIONS

3.1.2 Cantilever composite T-section model

The numerical composite material model developed in Section 2.4.1 is expanded to form a composite T-section part. This part has a fixed support on one side and a vertical load applied at the other, as a cantilever set-up. The model is then further advanced by bonding LEP to the underside of the composite T-section, which is representative of the final LEP bonded to a wind turbine blade and is shown in Figure 3 (a). Again, there is a cantilever set up with a vertical lead applied.

The maximum deformations of the composite T-section with and without LEP bonded to the underside are compared in Figure 3 (b), under a range of loadings from 1000-5000 N. For each of the models, the results of numerical simulations are compared to the theoretically predicted values, where the maximum deflection, y_{max}, can be calculated using:

$$y_{max} = \frac{FL^3}{3E}, \quad (2)$$

where, F is the vertical load applied at the end of the cantilever, L is the length of the cantilever, E is the Young's modulus and I is the moment of inertia of the cross section. As can be seen in Figure 3 (b), the difference between the results of the FEA model and the theoretically predicted values for a composite T-section with and without the LEP bonded to the underside is approximately 1% and 0.2%, respectively. The influence of the LEP bonded to the underside of the composite T-section increases the stiffness by approximately 3.5%.

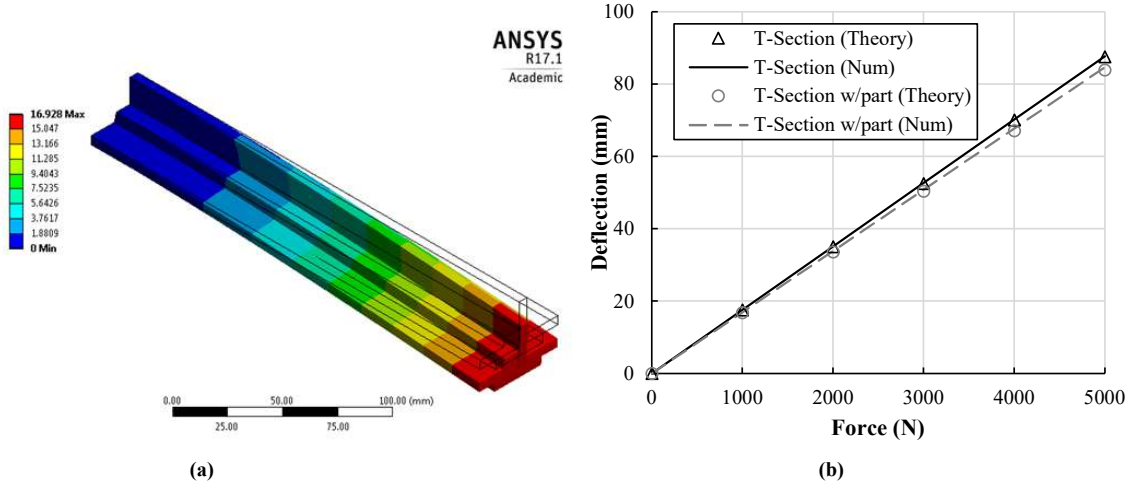

Figure 3: Numerical analysis of a cantilever composite T-section with LEP bonded to the underside, showing (a) the deformation (mm) for an end loading of 1000 N and (b) a comparison of the maximum deformation (mm) with the theoretical solution

https://doi.org/10.5194/wes-2020-20
Preprint. Discussion started: 31 March 2020

eawe european academy of wind energy
Open Access WIND ENERGY SCIENCE DISCUSSIONS

3.2 Leading edge demonstrator model validation

3.2.1 Demonstrator manufacture

In order to perform a validation study of the initial model of the LEP on a wind turbine blade, a leading edge demonstrator was manufactured. A summary of the four main manufacturing stages for the leading edge demonstrator are shown in Figure 4.

The demonstrator was designed based on the leading edge profile of the cross-section at 57 metres from the root of a commercial 63 metre blade, which is a blade form a 2.6 MW wind turbine that has a rotor diameter of 128 m. The profile is coupled with a rectangular base to form the cross-section of the demonstrator pattern. The demonstrator pattern has a continuous cross-section and was machined 5-axis CNC machine from multiple layers of polyurethane, where the final pattern is shown in the top left of Figure 4. A thermoset mould is then manufactured from this pattern using a glass-fibre reinforced high-temperature epoxy composite material, which is shown in the top right of Figure 4.

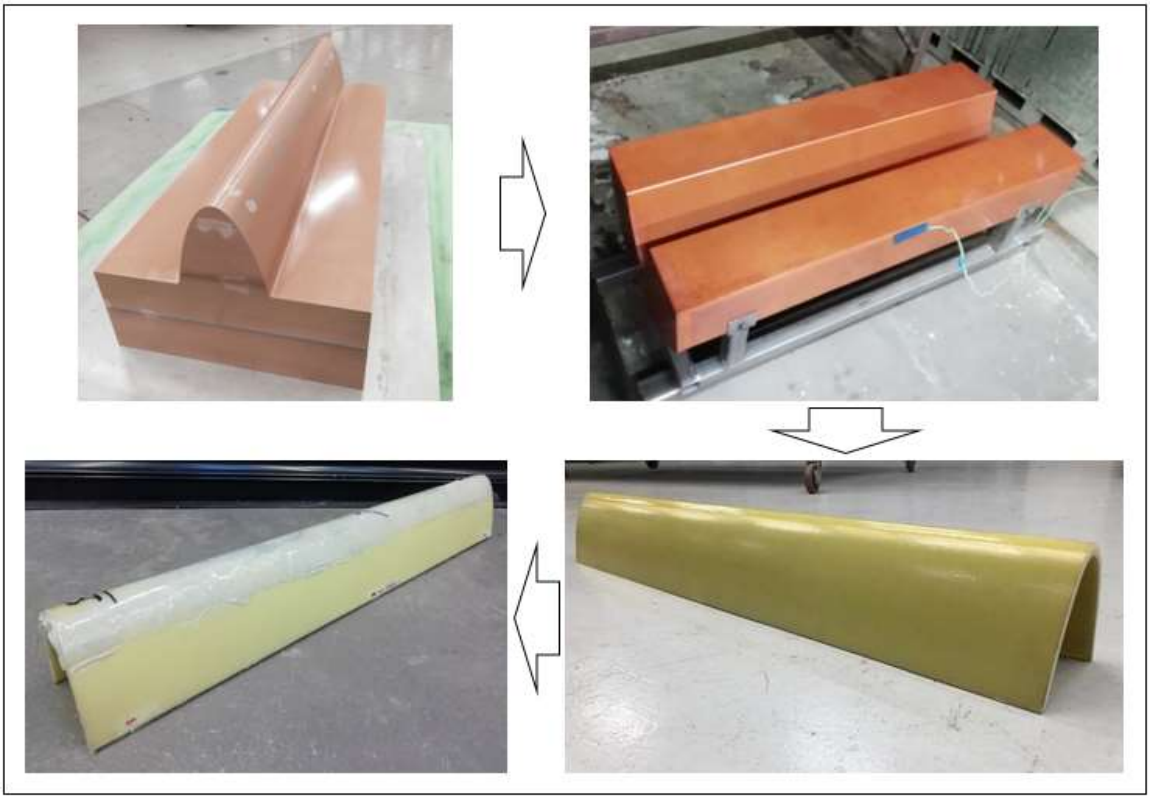

Figure 4: Summary of the main manufacturing stages for the demonstrator – from top left clockwise: demonstrator pattern; thermoset mould; powder epoxy glass fibre reinforced leading edge demonstrator; demonstrator with LEP bonded in place

https://doi.org/10.5194/wes-2020-20
Preprint. Discussion started: 31 March 2020

The blade substrate, which is made of glass-fibre reinforced powder epoxy composite material, was laid up on the mould. The layup is 1 layer of TRIAX (1.4mm thick), 8 layers of UD (0.9mm thick) and 1 layer of TRIAX (1.4mm thick) that are all orientated at 0° along the long edge of the demonstrator, which forms a part with a total thickness of 10mm. The LEP is then bonded to the blade substrate using an epoxy-based adhesive and cured at 70°C to form the final leading edge demonstrator, which is shown in the bottom left of Figure 4.

3.2.2 Demonstrator testing

The testing procedure for the leading edge demonstrator was a 4-point bending static test using the Denison 500 test machine at NUI Galway, where the test setup is shown in Figure 5. The demonstrator was simply supported at a spacing of 900 mm between the two supports and the static loading was applied vertically downwards in two places at a distance of 230 mm, where each loading point is 115 mm from the centre of the specimen. Initially, a number of trial specimens were tested in a similar set up to inform the final test campaign.

Figure 5: The leading edge demonstrator installed for a 4-point bending test in the Denison 500 test machine at NUI Galway

In order to obtain the required data, the demonstrator was instrumented with three linear electrical resistance strain gauges, which have a strain limit of approximately 5%, and one LVDT (linear variable differential transformer displacement sensor). The three strain gauges were located at the centre the demonstrator at the locations of highest strain and stresses - one at the

https://doi.org/10.5194/wes-2020-20
Preprint. Discussion started: 31 March 2020

top and one either side on the outside surface at the bottom – and the LVDT at the centre at the location of highest deflection, which can be seen in place in Figure 5.

Three tests, where the demonstrator was continuously loaded, were performed and the maximum load applied during the testing was 52.2kN. Failure in the demonstrator occurred at one of the support locations, where the internal support structure de-
200 bonded from the demonstrator substrate. However, no material failure within the demonstrator substrate was evident during or after the test.

3.2.3 Demonstrator FEA model analysis

The FEA model developed and validated in Section 3.1 is advanced in order to model the leading edge demonstrator, which was manufactured and mechanically tested. The blade substrate is defined using shell elements and the LEP is defined using
205 solid elements, where the contact region between the LEP and the blade surface is defined as a "bonded" connection, which restrains movement between the two surfaces in both the normal and tangential direction. The layup for the blade substrate is the same as the layup specified in Section 3.2.1, which is specified at the shell elements using the "Layered Section" in ANSYS Mechanical ADPL, and the material properties specified in the FEA model are those given in Table 1. The mesh for the computation domain has a specified maximum element size of 10 mm, resulting in a mesh containing 15,100 elements with
210 27,500 nodes. The computational domain for the demonstrator FEA model is shown alongside the leading edge demonstrator in Figure 6. Displacement restraints have been specified at the two support points to model a simply supported system and two point loads have been specified, in order to represent a 4-point bending static test, which was performed on the leading edge demonstrator in Section 3.2.2.

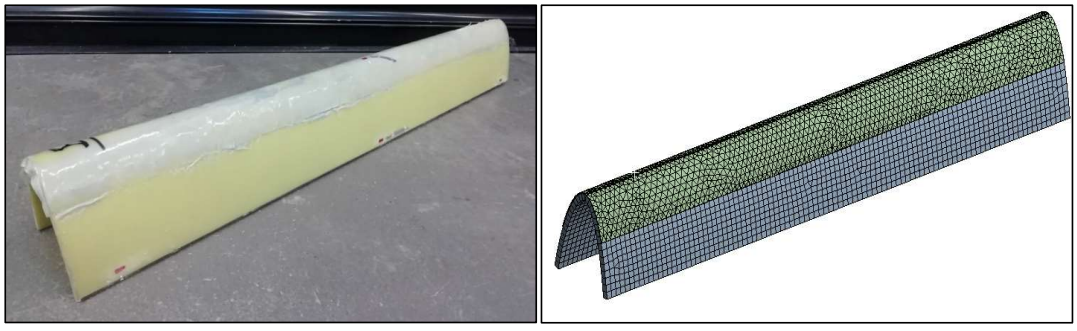

215 **(a)** **(b)**

Figure 6: Leading edge demonstrator used for the validation study, showing (a) the physical model used for the experimental trials and (b) the meshed geometry used in the numerical FEA model

https://doi.org/10.5194/wes-2020-20
Preprint. Discussion started: 31 March 2020

eawe european academy of wind energy
Open Access WIND ENERGY SCIENCE DISCUSSIONS

3.2.4 Demonstrator FEA model validation

The results of the experimental testing, which is discussed in Section 3.2.2, have been compared to the results from the FEA model of the leading edge demonstrator. A comparison between the two sets of results for vertical load applied against the maximum deflection of the demonstrator is shown in Figure 7. The FEA model under-estimates the deflection occurring during the testing but is in reasonable agreement. The strain occurring during the testing was monitored at three locations along the centre of the demonstrator, which can be seen in Figure 5. The FEA model over-estimates the level of strain occurring but the directionality is constant, which can been in Figure 8. Overall, there is reasonable agreement between the two sets of results. The FEA model is then used to examine the frictional stress between the LEP and the blade substrate a loading of 40 kN. The maximum frictional stress is 6.4 MPa, as shown in Figure 9 (b). This occurs at the contact points of the loading mechanism, which would not happen in operation. Contour plots showing the deflection and Von Mises (equivalent) stress are also shown in Figure 9 (a).

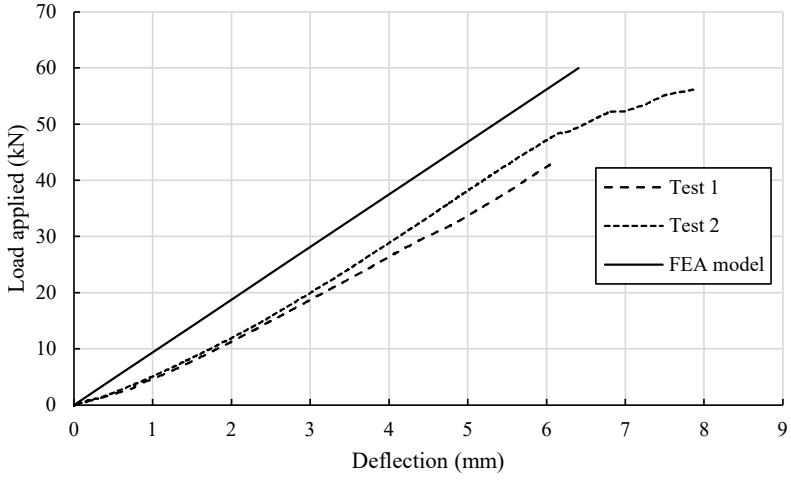

Figure 7: Deflection (mm) of the centre of the specimen against load (kN) applied during the testing (data for Test 3 not available)

https://doi.org/10.5194/wes-2020-20
Preprint. Discussion started: 31 March 2020

eawe european academy of wind energy
Open Access WIND ENERGY SCIENCE DISCUSSIONS

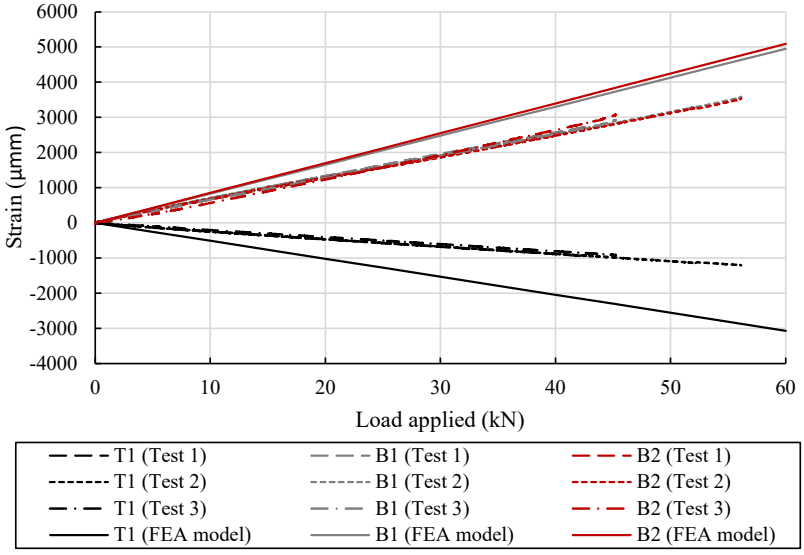

Figure 8: Strain recorded by the 3 linear strain gauges at the centre of the demonstrator during each test

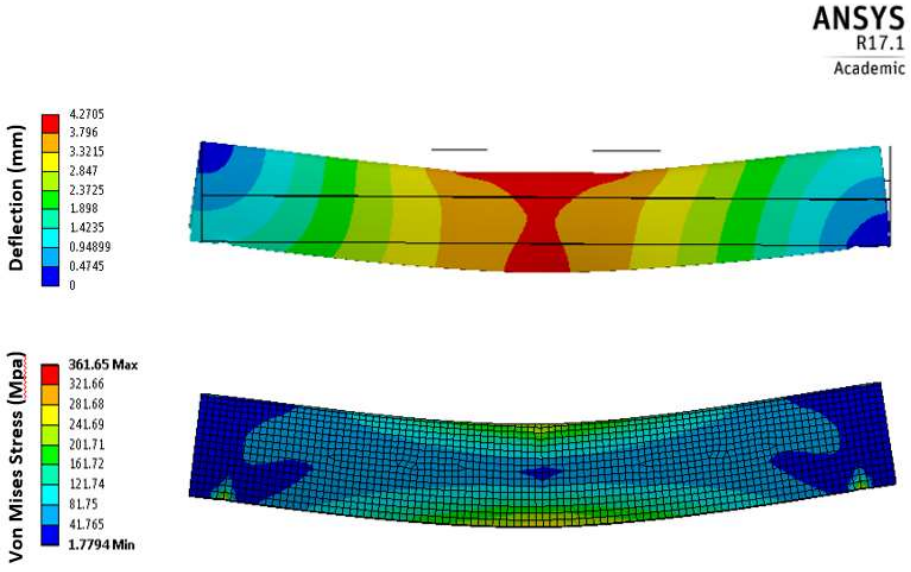

235 **(a)**

https://doi.org/10.5194/wes-2020-20
Preprint. Discussion started: 31 March 2020

eawe european academy of wind energy
Open Access WIND ENERGY SCIENCE DISCUSSIONS

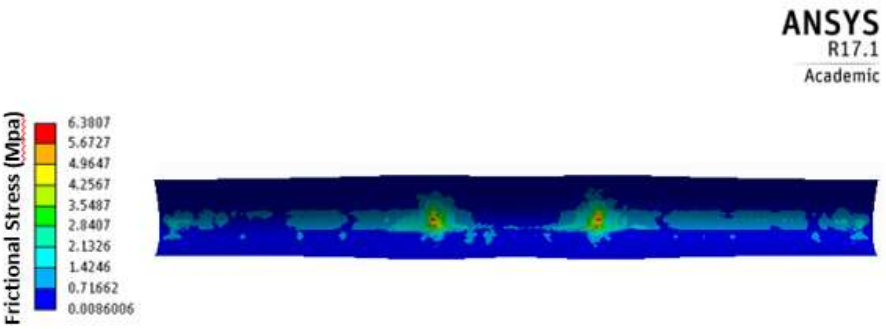

(b)

Figure 9: Contour plots showing the results from the FEA model when a loading of 40 kN is applied to the demonstrator, where (a) is the deflection and Von Mises (equivalent) stress and (b) is the frictional stress between the LEP and the blade substrate

3.3 Full-scale wind turbine blade model

The validated FEA model is then applied to a full-scale (13 metre) wind turbine blade with a LEP bonded to the leading edge of along the 8 metres towards the tip.

3.3.1 Model details

The full-scale wind turbine blade is a 13-metre long blade from a 225 kW wind turbine, which has a total mass of approximately 800 kg. The blade is manufactured from glass-fibre reinforced powder epoxy composite material using a novel "one-shot" manufacturing process, which cures the different parts of a wind turbine blade (i.e. skin sections, spar caps web and root) in one single process to avoid the need for gluing. Steel inserts in the root of the blade provide a connection to the turbine hub, which will be modelled as a "fixed support" at the root within the FEA model. An 8-metre long LEP is attached to the leading edge of the blade towards the tip. This is shown in yellow in the meshed geometry in Figure 10. The LEP is a thermoplastic polyurethane that has been selected due to its high tolerance to rain erosion and UV resistance. The main components of the wind blade (shell, spar, web) were defined using shell elements, where the composite layup is defined using the material properties, thickness of each play and the ply orientation, and the LEP is defined using a solid region extruded from the blade surface along the leading edge. Similar to the precious section, the contact region between the LEP and the blade surface is defined as a bonded connection.

The blade is manufactured from three materials, UD, TRIAX and PU core, which are described in detail in Section 2.4, and their material properties are given in Table 1. The main structural element of the blade is the spar caps, which are primarily manufactured from UD plies that are orientated along the length of the blade, and shear webs, which are manufactured from both UD and TRIAX plies that are also orientated along the length of the blade. Each of the plies have a thickness of approximately 1 mm. The composite ply layup details for the wind turbine blade have been detailed in Table 2.

https://doi.org/10.5194/wes-2020-20
Preprint. Discussion started: 31 March 2020

eawe european academy of wind energy
Open Access WIND ENERGY SCIENCE DISCUSSIONS

A maximum element size was specified of 200 mm when creating the mesh for the computation domain, which is shown in Figure 10. This resulted in a mesh containing 52,500 elements with 90,600 nodes.

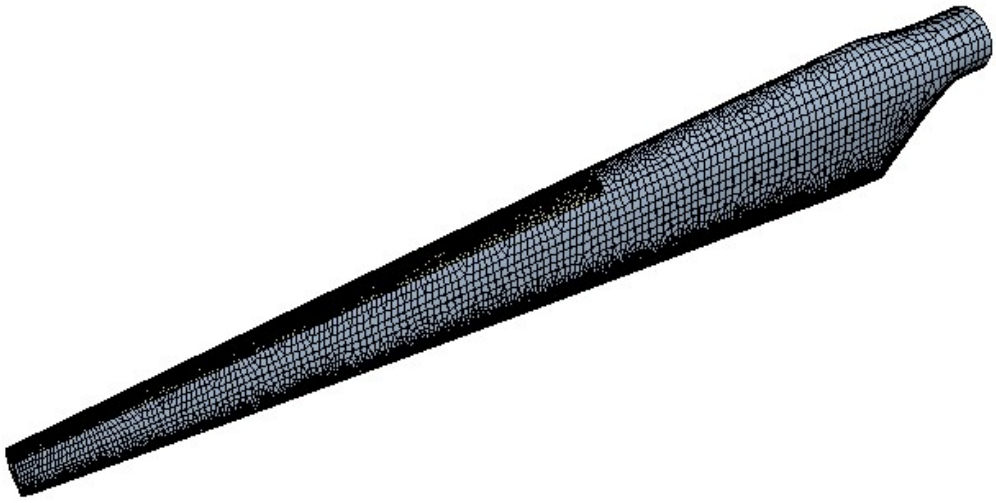

Figure 10: Meshed geometry (computational domain) used for the FEA of the full-scale wind turbine blade with LEP bonded to the leading edge (as shown in yellow)

Table 2: Details of the composite ply layups for the full-scale wind turbine blade

Blade length (m)	Shell (leading edge)			Shell (trailing edge)			Spar caps + shell			Web		
	TRIAX	UD	Core	TRIAX	UD	Core	TRIAX	UD	Core	TRIAX	UD	Core
0.5	4	4	1	2	4	1	2	16	1	2	4	
1	4	4	1	2	4	1	2	16	1	2	4	
1.5	4	4	1	2	4	1	2	16	1	2	4	
2	4	2	1	2	2	1	2	16	1	2	2	
2.5	4	2	1	2	2	1	2	16	1	2	2	
3	4	2	1	2	2	1	2	16	1	2	2	
3.5	4	2	1	2	2	1	2	16	1	2	2	
4	4	2	1	2	2	1	2	16	1	2	2	
4.5	4	2	1	2	2	1	2	16	1	2	2	
5	4	2	1	2	2	1	2	14	1	2		
6	4	2	1	2	2	1	2	14	1	2		
7	4	2	1	2	2	1	2	14	1	2		
8	4	2	1	2	2	1	2	14	1	2		
9	4	2	1	2	2	1	2	14	1	2		
10	4	2	1	2	2	1	2	14	1	2		
11	4	2	1	2	2	1	2	14	1	2		
12	4	2	1	2	2	1	2	14	1	2		
13	5			3			2	14	1	2		

https://doi.org/10.5194/wes-2020-20
Preprint. Discussion started: 31 March 2020

eawe european academy of wind energy
Open Access WIND ENERGY SCIENCE DISCUSSIONS

3.3.2 FEA model analysis

In order to ensure the accuracy of the FEA model and the wind turbine blade set-up, the results (blade deflection) from the FEA model are compared to the experimental trials performed by Fagan et al. (2017) for the same blade. The loading used in the experimental trials was defined from the maximum expected wind loading on the blade in operation and this same loading is used within the analysis presented in this study. In this study, the loading was applied as three point loads along the blade, which were specified as 7.32 kN at 5m from the blade root, 3.38 kN at 10m from the blade root and 2.3 kN at 12m from the blade root (1 m from the tip of the blade).

The deflection of the blade that is predicted in the FEA model (seen in Figure 11) agrees well with the results from the experimental trials performed in Fagan et al. (2017), which can be seen in Figure 12. The mechanical performance of the LEP component during operation is not expected to contribute to the mechanical performance of the wind blade. However, based on the comparative results in Figure 12 for the wind blade with and without the LEP attached, the addition of the LEP increases the stiffness of the blade. Nevertheless, it is essential that the von Mises stresses on the component are lower than the allowable stress of the materials used for the LEP component.

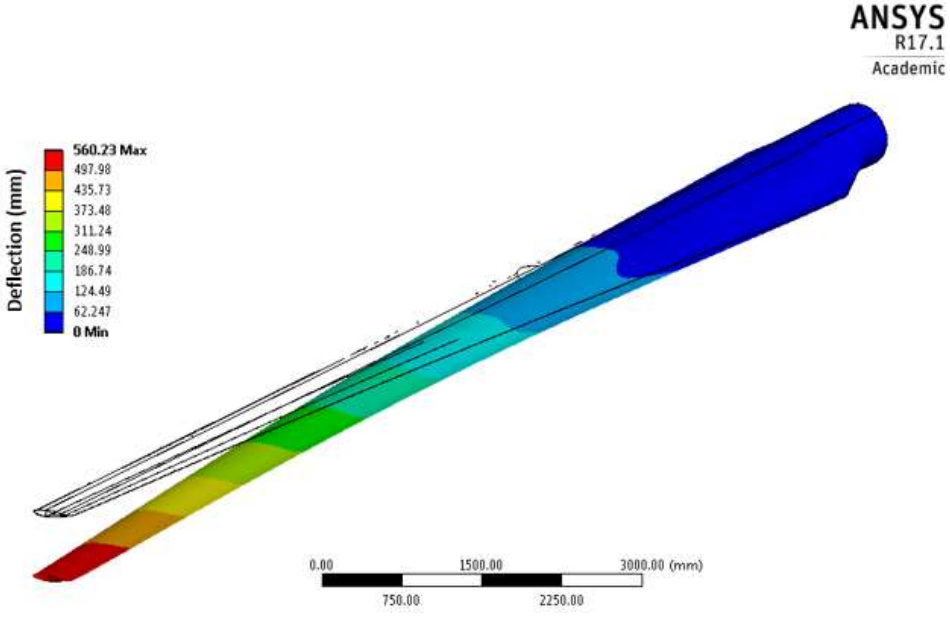

Figure 11: Deflection of the FEA model of the full-scale wind turbine blade under the defined loading

https://doi.org/10.5194/wes-2020-20
Preprint. Discussion started: 31 March 2020

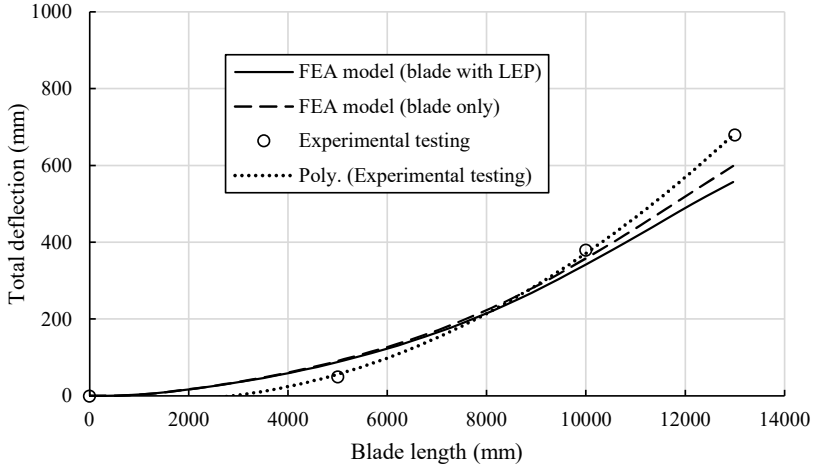

Figure 12: Comparison of the deflections from the FEA model of the full-scale wind turbine blade under the defined loading along the length of the blade with and without the LEP bonded and the experimental results (Fagan et al., 2017)

285

The von Mises (equivalent) stress on the blade is shown in Figure 13 when the defined loading is the same as in the experimental trials performed in Fagan et al. (2017). The highest stresses are along the spar caps at 1.3 m from the root of the blade of up to 200 MPa. This value is well below the maximum allowable stress for the blade substrate of 643 MPa, which is the compressive strength of UD glass fibre reinforced powder epoxy mechanically tested at an orientation of 0^0. The tensile
290 strength of UD glass fibre reinforced powder epoxy when mechanically tested at an orientation of 0^0 was found to be 782 MPa. The von Mises stress imposed within the LEP material is 2.6 MPa throughout the component except for a concentrated high stress area near the tip of the blade, where the stresses are above the yield strength of the material (6 MPa). The frictional stress along the bonded contact between the blade substrate and the LEP component was found to be 32.8 MPa except for a concentrated high stress area, again, near the tip of the blade, where the frictional stress reaches 82 MPa. This is higher than
295 the maximum tensile stress of the epoxy adhesive of 49 MPa. This high stress area near the tip, will need to be addressed in the component design and manufacture stages of development.

https://doi.org/10.5194/wes-2020-20
Preprint. Discussion started: 31 March 2020

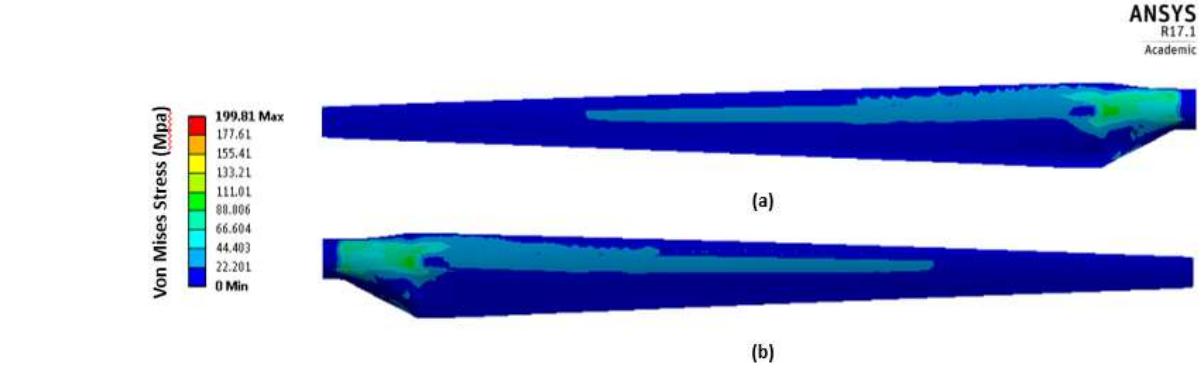

Figure 13: Contour plots showing the Von Mises (equivalent) stress from the FEA model of the full-scale wind turbine blade under the defined loading

4 Conclusion

An advanced FEA model of a new leading edge protection component (LEP) for wind turbine blades has been developed in this study. The FEA model has been validated against experimental trials at demonstrator level, comparing the deflection and strains during testing and found to be in good agreement. A full-scale wind turbine blade is then modelled with the LEP bonded onto the blade's leading edge and compared to previously performed experimental trials (Fagan et al., 2017), where the results were found to be well aligned when comparing the deflections of the blade.

The methodology used to develop the FEA model can be applied to other wind blade designs in order to incorporate the new LEP as a protection from rain erosion along the leading edge of the blade. The results of the model will allow engineers to explore the effect of the new LEP on their existing wind blades, including the blade stiffness, von Mises stress on the blade and frictional stress at the bond.

The structural integrity of wind blades in the offshore environmental is paramount in the success of the sector. Regular maintenance will prove much more difficult and costly offshore, compared to onshore wind installations. A robust leading edge protection system that protects the blade from rain erosion for the duration of its life span will significantly reduce the need for maintenance and, in turn, increase the reliability and service life of the blades.

Data availability

Publicly available testing data available in this publication. Additional testing data may be granted through contact with William Finnegan.

https://doi.org/10.5194/wes-2020-20
Preprint. Discussion started: 31 March 2020

eawe european academy of wind energy
Open Access WIND ENERGY SCIENCE DISCUSSIONS

Author contribution

William Finnegan: Conceptualization, Data curation, Investigation, Methodology, Formal analysis, Writing - Original Draft. **Priya Dasan Keeryadath**: Data curation, Investigation. **Rónán Ó Coistealbha**: Data curation, Investigation. **Tomas Flanagan**: Supervision, Conceptualization, Funding acquisition. **Michael Flanagan**: Conceptualization, Project administration. **Jamie Goggins**: Supervision.

Competing interests

The authors declare that there are no conflicts of interest.

Acknowledgments

This study was funded by the Executive Agency for Small and Medium sized Enter-prises (EASME) in the European Commission through the LEAPWind project (Agreement no.: EASME/EMFF/2017/1.2.1.12/S1/06/SI2.789307). The study was also funded in part by Sustainable Authority of Ireland (SEAI) through the SEAI Research, Development and Demonstration Finding Programme 2019 through the BladeLEP project (Grant no. 19/RDD/430). The first and last authors would like to acknowledge the support from Science Foundation Ireland (SFI), through the Marine and Renewable Energy Ireland (MaREI) research centre (Grant no. 12/RC/2302),

https://doi.org/10.5194/wes-2020-20
Preprint. Discussion started: 31 March 2020

eawe european academy of wind energy
Open Access WIND ENERGY SCIENCE DISCUSSIONS

References

Agarwal, B.D., Broutman, L.J., Chandrashekhara, K., 2017. Analysis and performance of fiber composites. John Wiley & Sons.

ANSYS, 2017. ANSYS® CFX (Release 17.1): CFX-Solver Theory Guide, . ANSYS Inc.

ASTM, 2017. D3039 / D3039M-17: Standard test method for tensile properties of polymer matrix composite materials. ASTM International, West Conshohocken, PA, USA.

Barnes, R.H., Morozov, E.V., Shankar, K., 2015. Improved methodology for design of low wind speed specific wind turbine blades. Composite Structures 119, 677-684.

Bo, Z., YU, F.-a., 2016. Finite Element Analysis of Wind Turbine Blades. DEStech Transactions on Computer Science and Engineering.

Budinski, K.G., 2007. Guide to friction, wear and erosion testing. ASTM international West Conshohocken, USA.

Chen, J., Wang, J., Ni, A., 2019. A review on rain erosion protection of wind turbine blades. Journal of Coatings Technology and Research 16, 15-24.

Conway, J., 2015. World wind power to almost double to 650GW by 2020, The Australian.

Cortés, E., Sánchez, F., O'Carroll, A., Madramany, B., Hardiman, M., Young, T.M., 2017. On the material characterisation of wind turbine blade coatings: the effect of interphase coating–laminate adhesion on rain erosion performance. Materials 10, 1146.

Dashtkar, A., Hadavinia, H., Sahinkaya, M.N., Williams, N.A., Vahid, S., Ismail, F., Turner, M., 2019. Rain erosion-resistant coatings for wind turbine blades: A review. Polymers and Polymer Composites 27, 443-475.

El Chazly, N.M., 1993. Static and dynamic analysis of wind turbine blades using the finite element method. Renewable Energy 3, 705-724.

Fagan, E.M., Flanagan, M., Leen, S.B., Flanagan, T., Doyle, A., Goggins, J., 2017. Physical experimental static testing and structural design optimisation for a composite wind turbine blade. Composite Structures 164, 90-103.

Finnegan, W., Flanagan, T., Goggins, J., 2020. Development of a Novel Solution for Leading Edge Erosion on Offshore Wind Turbine Blades, in: Wahab, M.A. (Ed.), Proceedings of the 13th International Conference on Damage Assessment of Structures. Springer Singapore, Singapore, pp. 517-528.

Gurit, Ampreg 22: Epoxy Laminating System Datasheet.

Keegan, M.H., Nash, D.H., Stack, M.M., 2013. On erosion issues associated with the leading edge of wind turbine blades. Journal of Physics D: Applied Physics 46, 383001.

Kennedy, C.R., Jaksic, V., Leen, S.B., Brádaigh, C.M.Ó., 2018. Fatigue life of pitch- and stall-regulated composite tidal turbine blades. Renewable Energy 121, 688-699.

Lopes, C.S., González, C., Falcó, O., Naya, F., Llorca, J., Tijs, B., 2016. Multiscale virtual testing: the roadmap to efficient design of composites for damage resistance and tolerance. CEAS Aeronautical Journal 7, 607-619.

SEIMENS, 2019. Siemens Gamesa launches 10 MW offshore wind turbine; annual energy production (AEP) increase of 30% vs. predecessor. SEIMENS Gamesa Newroom.

Tarfaoui, M., Nachtane, M., Boudounit, H., 2019. Finite Element Analysis of Composite Offshore Wind Turbine Blades Under Operating Conditions. Journal of Thermal Science and Engineering Applications 12.

Yeh, M.-K., Wang, C.-H., 2017. Stress analysis of composite wind turbine blade by finite element method, IOP Conference Series: Materials Science and Engineering. IOP Publishing, p. 012015.

Zhu, S.F., Rustamov, I., 2013. Structural design and finite element analysis of composite wind turbine blade, Key Engineering Materials. Trans Tech Publ, pp. 225-228.